Heliyon 8 (2022) e09930

Contents lists available at ScienceDirect

Heliyon

journal homepage: www.cell.com/heliyon

Research article

# Activated carbon derived from waste orange and lemon peels for the adsorption of methyl orange and methylene blue dyes from wastewater

Denga Ramutshatsha-Makhwedzha *, Avhafunani Mavhungu, Mapula Lucey Moropeng, Richard Mbaya

*Department of Chemical, Metallurgical and Materials Engineering, Tshwane University of Technology, Pretoria West Campus, Private Bag X680, South Africa*

ARTICLE INFO

*Keywords:*
Orange lemon peel activated carbon (OLPAC)
Methylene blue
Methyl orange adsorption
Wastewater

ABSTRACT

The study of adsorbent behaviour in laboratory conditions helps to predict the adsorption process in a large industrial scale. In this study, orange and lemon peels-derived activated carbon (OLPAC) was successfully synthesized and activated using phosphoric acid. Characterization was performed on the OLPAC and the material was used for the removal of methyl orange (MO) and methylene (MB) dyes from wastewater. The results of the scanning electron microscope and $N_2$ adsorption/desorption examination affirmed that the prepared nanocomposite is permeable, which is an advantage for the efficient removal of contaminants. Optimal conditions for the batch removal process were investigated using a one-factor time approach in different conditions of adsorption (Dye concentration 50–200 mg $L^{-1}$, pH 2–10, adsorbent mass 0.010–0.8, and contact time 5–180 min. The adsorption isotherm equilibrium data were examined by Langmuir, Freundlich, and Temkin, isotherm model. As shown by the correlation coefficient ($R^2$), the data were best described by Langmuir isotherms with maximum adsorption capacities of 33 and 38 mg $g^{-1}$ for methyl orange and methylene blue, respectively. Adsorption kinetic data were described using the pseudo-second-order model which suggests that adsorption of MO and MB was by chemisorption mechanism. The method was applicable to real wastewater samples, with satisfactory removal percentages of OM and MB (96 and 98 %). The results of this study show that OLPAC is an inexpensive biosorbent that is successfully utilized in removing methyl orange and methylene blue dyes from wastewater.

## 1. Introduction

The release of large amounts of pollutants into the environment due to the rapid increase in industrial and agricultural activities is one of the key challenges globally (Ahmadi and Ganjidoust, 2021). Dyes are a type of pollutant that must be extricated from wastewater before being released into the natural habitat due to toxicity and negative effects on photosynthetic activity (Çatlıoğlu et al., 2021; Wong et al., 2018).

Dye effluents discharged into the aquatic environment increase the color saturation of the receiving water and prevent sunlight from entering the water. As a result, these will harm aquatic life (Cheng et al., 2022). The most widely used dye in the textile industry is methylene blue, which is used for dyeing and finishing fabrics. In any case, too much exposure to methylene blue is harmful to people and oceanic life as it can cause skin sensitivities, sensory system issues, and at last cardiovascular harm (Parlayıcı and Pehlivan, 2021). Malachite green is another type of dye commonly used in the textile and leather industries that can cause harm to the human respiratory tract and may potentially be capable of causing liver tumors (Hijab et al., 2021; Kooravand et al., 2021). Its release into the water stream must be strictly managed to prevent it from causing many significant environmental problems and harmful hazards.

Wastewater treatment techniques, for example, membrane filtration, ion exchange, coagulation, advanced oxidation processes, and adsorption, were used for the removal of dyes (Ahmadi and Ganjidoust, 2021; Çatlıoğlu et al., 2021).

Amidst these techniques, adsorption has great decontamination potential due to its tunability, versatility, and a wide variety of available sorbents (Dimpe and Nomngongo, 2017; Mashile et al., 2021). The efficiency of the adsorption technique is strongly reliant on the characteristics of the analyte, type of the adsorbent, and wastewater matrix composition (Mashile et al., 2021). Recent research has focused on finding cost-effective, efficient, and environmentally friendly adsorbents for the removal of dyes as well as optimizing the adsorption process

* Corresponding author.
*E-mail address:* makhwedzhad@tut.ac.za (D. Ramutshatsha-Makhwedzha).

https://doi.org/10.1016/j.heliyon.2022.e09930
Received 15 March 2022; Received in revised form 2 April 2022; Accepted 7 July 2022

(Ngah et al., 2011; Olivera et al., 2016; Singh et al., 2018; Tan et al., 2012; Wong et al., 2018; Yagub et al., 2014).

The most generally utilized adsorbent material is activated carbon, but its frequently expensive to produce and includes the utilization of activating agents which can leach into solution and cause secondary pollution (Çatlıoğlu et al., 2021). Lately, numerous scientists have explored the use of activated carbon derived from natural and low-cost agricultural wastes such as banana peels, orange peels, lemon peels, peanut shells, bamboo shoots, and coconut shells for the removal of dye contaminants from water (Ahmadi and Ganjidoust, 2021; Hashem et al., 2020; Jiang et al., 2021; Wong et al., 2018).

One of the possible low-cost adsorbents is orange/citrus peel. In addition, fruit peels or skins generally consist of lignin, cellulose, hemicellulose, carboxyl, hydroxyl, pectin substances, and amide surface functional groups which enhances the adsorbent-adsorbate interactions (Pandiarajan et al., 2018). World citrus production was almost 140 million tons and growing, and orange production was reported to be 70 million tons in 2015 (Gunay Gurer et al., 2021). Both lemon and orange peel are no longer useful after the juice extraction and is free of charge from the processing industry, therefore, it is a preferred sorbent that has been studied by many researchers (Ahmed et al., 2020; Bukhari et al., 2022; Eddy et al., 2022; Zhang et al., 2022). Citrus peels as market waste cause disposal problems in terms of environmental impact.

As a results, carbon-rich agricultural residues will contribute to the negative environmental impacts when landfilled due to leachate that could lead to greenhouse gas emissions. Hence of, the manufacture of AC from waste materials, particularly agricultural residues would add economic value, reduce the cost and waste, and provide an economical alternative to commercial ACs.

In this study, orange and lemon peels/skins were selected as precursors to prepare porous activated carbon to get rid of methylene blue (MB) and methyl orange (MO) dyes from wastewater. The conversion of biowaste to highly orange lemon peel activated carbon (OLPAC) using $H_3PO_4$ is cost-effective and eco-friendlier as compared to the use of other commercially available carbon adsorbents. All adsorption experiments were performed using ultrasonic irradiation. When ultrasonic irradiation is applied, the interaction between the solute and the adsorbent is promoted, and mass transfer on the surface of the material is promoted, thus improving the adsorption efficiency (Çatlıoğlu et al., 2021; Mashile et al., 2021). In the literature, the effects of ultrasonic irradiation on the adsorption of various contaminants from aqueous solutions have been documented (Geaneth Pertunia et al., 2020; Gugushe et al., 2021; Madimetja and Nomngongo, 2019; Mpupa et al., 2020; Ramutshatsha-Makhwedzha et al., 2019).

Activated carbon made from both lemon and orange peels (1:1) is applied for the first time in batch adsorption of MB and MO dye with phosphoric acid as an activating agent. The effect of various conditions such as pH, adsorbent mass, and contact time on the performance of the method was evaluated and the optimal conditions were used to evaluate the method of isotherms and kinetics models.

## 2. Experimental

### 2.1. Materials and reagents

Orthophosphoric acid, 98 %, nitric acid ($HNO_3$), sodium nitrate ($NaNO_3$), and sodium hydroxide (NaOH) were purchased from Ace, Arkema and Merck (Johannesburg, South Africa), respectively. Methyl orange (Rochelle Chemicals, Johannesburg, South Africa) and methylene blue (Ace, Johannesburg, South Africa) are analytical grades. 1000 mg $L^{-1}$ of dye stock solution was made with redistilled water and diluted as needed to make a working solution.

### 2.2. Instrumentation

The adsorbent was characterized using Fourier Transform Infrared (FTIR) spectroscopy (Perkin Elmer Spectrum 100 spectrometer) and identified functional groups. The specific surface area and material pore distribution of the Brunauer-Emmett-Teller (BET) were analyzed using ASAP2020 V3. 00H Micromeritics Instrument (Norcross, Georgia, USA). A scanning electron microscope linked to energy-dispersive X-ray spectroscopy (SEM, JSM-6360LVSEM, JEOL Co., Japan) examined morphology and nanostructure synthetic materials. X-ray diffraction (XRD) studies were performed using PANalytical X'Pert Xray Diffractometer to evaluate the crystallinity of the adsorbent. Charge (pHpzc) of OLPAC was examined using a method modified in the literature (Akawa et al., 2021b).

### 2.3. Preparation of activation carbon adsorbent

The activated carbon was synthesized following a modified method (Fernandez et al., 2014). Briefly, orange and lemon skins were collected from a fresh market, thoroughly washed with deionized water, and separately dried in the oven at 110 °C for 24 h. The dried skins were then pulverized into small particles, sizes ranging from 200 – 400 μm. Equal amounts of orange and lemon skins were mixed and properly homogenized before impregnation with an equal volume of 85 % $H_3PO_4$. The excess liquid was removed, and the material was dried for 24 h in the oven at 110 °C. Thereafter, the carbon was placed in a furnace at 600 °C for 3 h. The chemically activated carbon was cleansed using distilled water and dried at 110 °C. The orange-lemon peel-activated carbon is henceforth referred to as OLPAC.

### 2.4. Adsorption experiments

A one at a time factor optimization strategy was utilized in determining the optimal experimental conditions. Briefly, the batch adsorption experiments were done as follows: A 50 mL of the model solution containing a 100 mg $L^{-1}$ concentration of the dyes was added to a glass vessel and the pH of the solution was adjusted with dilute $HNO_3$ or NaOH. The pH studied ranged from 2 to 10. Thereafter, a predetermined amount of the adsorbent (0.010–0.8 g) was mixed to the solution before sonication at ambient temperature for 5–180 min. The supernatant was centrifuged at 2000 rpm for 3 min using a UV-vis spectrophotometer (Aqualytic AL800 Portable Spectrophotometer, Germany) at $\lambda$max of each dye. The results are averages of minimum of 3 experiments.

The adsorbed amount of MO and MB onto the sorbent was calculated using Eq. (1):

$$Adsorption\ \ capacity\ q_e = \frac{(C_o - C_e)}{m}\nu \tag{1}$$

Where $q_e$ is the amount of the adsorbate that was adsorbed in mg $g^{-1}$, $C_o$ and $C_e$ are the initial and equilibrium concentrations of dye in water after removal process (mg $L^{-1}$), respectively, V is the solution volume (L) and m is the amount of OLPAC material (g).

The adsorption efficiency (% RE) was used as the analytical response using Eq. (2).

$$Adsorption\ \ efficiency = \frac{C_o - C_e}{C_o} \times 100 \tag{2}$$

Finally, kinetic and isotherm studies were performed under optimum conditions for each dye to determine the adsorption reaction characteristics. Kinetic studies were performed by varying the exposure time from 5 to 180 min, while adsorption isotherms were studied at initial dye concentrations of 50–200 mg $L^{-1}$. Tables 1 and 2 shows equations of these models and they are widely reported from literature (Cheng et al., 2022; Gugushe et al., 2021; Mashile et al., 2021; Mpupa et al., 2020).

Adsorbent regeneration was achieved by continuous washing under ultrasound for 5 min with 3 M $HNO_3$ and deionized water and drying before the next use.

**Table 1.** Isotherms models with their parameters.

| Isotherms model | Linear equation | Parameters |
|---|---|---|
| Langmuir Isotherm | $\frac{C_e}{q_e} = \frac{1}{q_{max}}C_e + \frac{1}{K_L q_{max}}$ | The $q_{max}$ and $K_L$ are Langmuir constant relating the adsorption capacity (mg $g^{-1}$) and energy of adsorption (L $g^{-1}$). |
| Freundlich Isotherm | $\ln q_e = \ln K_F + \frac{1}{n}\ln C_e$ | $K_F$ is the Freundlich constant which relates to adsorption capacity and 1/n is the adsorption intensity. |
| Temkin | $q_e = B_1 \ln K_T + B_1 \ln C_e$ | $B_T$ is heat of adsorption (J $mol^{-1}$). $K_T$ is isotherm constant relating to binding equilibrium ($Lg^{-1}$) |

**Table 2.** Kinetics models and their parameters.

| Kinetics model | Linear equation | Parameters |
|---|---|---|
| Pseudo-1st order | $\ln(q_e - q_t) = lnq_e$ | Where $q_t$ is adsorption capacity at time t (mg $g^{-1}$), $k_1$ |
| Pseudo-2nd order | $\frac{t}{q_t} = \frac{1}{k_2 q_e^2} + \frac{1}{q_e}t$ | $k_2$ are the rate constant (g mg $min^{-1}$) |
| Intra-particle diffusion | $q_t = k_d t^{1/2} + c$ | $k_d$ are the rate constant (mg g $min^{-1/2}$) |

### 2.5. Application to wastewater

Wastewater samples were collected from laboratory wastewater based in Pretoria West campus (Gauteng, South Africa). About 500 ml of wastewater samples were stored in polyethylene bottles and refrigerated at 4–8 °C. To prevent any possible contamination, polyethylene bottles were first cleaned and socked in $HNO_3$ (1%) and thereafter cleansed with distilled water.

## 3. Results and discussion

### 3.1. Physico-chemical properties of the adsorbents

The functional groups available on the OLPAC were analysed by FTIR spectroscopy. The spectrum of the OLPAC adsorbent displayed in Figure 1 shows that the most commonly identified functional group in OLPAC are: –CH, –OH, –C–O, –COO, and –C=O. The wide peaks at 3280 $cm^{-1}$ were ascribed to the O—H groups vibrations of carboxylic acid, alcohols, and phenols, and the peak of 2869 $cm^{-1}$ was assigned to the $CH_2$ stretch. Additionally, the 1570 $cm^{-1}$ and 1387 $cm^{-1}$ bands were assigned to the C = O and C = C stretches of the carboxyl and carbonyl groups, respectively. A faint peak of 1022 $cm^{-1}$ was assigned to the C–O stretching vibrations (Akawa et al., 2021a; Dey et al., 2021; Pandiarajan et al., 2018).

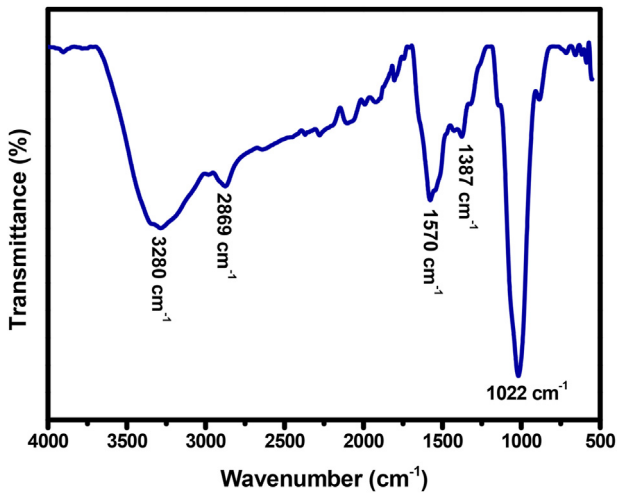


**Figure 1.** FTIR spectrum of OLPAC.

The BET surface area, pore volume, pore size of OLPACs investigated using $N_2$ adsorption/desorption isotherms are 0.269 $m^3\ g^{-1}$, 5.18 nm and 168.29 $m^2$, respectively. $g^{-1}$. The $N_2$ desorption isotherms and pore size distribution curves of the OLPAC materials are displayed in Figure 2 (a) and (b). The isotherms show a type IV isotherm with hysteresis ring H1, specifying the neutral nature of the adsorbent (Hassan et al., 2014; Nasrullah et al., 2018). As shown in Figure 2 (b), the average pore size of the material is about 5.18 nm, and most pores represents the mesoporous structure corresponding to the pore size of the IUPAC classification, that confirms the mesoporous properties. The mesoporous structure and a huge specific surface area of OLPAC suggest a high adsorption capacity towards the targeted adsorbates.

The crystal phase and microstructure of the prepared OLPAC were confirmed by XRD and the diffractographic pattern from the XRD (**Figure 3(a)**) displays two peaks at 2θ = 22.8°and 43.8°. These peaks were ascribed to the (0 0 2) and (1 0 0) that resembles the disordered carbon sheet (Li et al., 2016). The wide diffraction peaks indicated that the synthesized material was amorphous. The surface morphology and elemental composition of the OLPAC were investigated using SEM-EDS and the images and spectrum are displayed in Figure 3 (b) – (d). As seen from the SEM images in Figure 3(b)–(c) a highly porous material, with surface pores, was successfully synthesized. This porous structure allows efficient adsorption as it offers adequate free spaces for target adsorbates (Akawa et al., 2021a). The EDS spectrum of the prepared material in Figure 3(d) confirmed the availability of mainly C and O. The presence of P was attributed to the phosphoric acid activation agent.

### 3.2. Evaluation of the adsorption characteristics of activated carbon

#### 3.2.1. Adsorption experiment studies

The pH of the solution is one of the most significant parameters which affect the adsorption of dyes because solution pH controls the adsorbent-adsorbate interactions (Baloo et al., 2021). It is therefore important to optimize and determine the optimum pH conditions. Figure 4(a) shows the removal efficiencies of the MO and MB dyes on the OLPAC with varying pH (2–10). It can be observed from the graphs that the removal efficiency of MO was highest at pH 2 (94 %) and drastically decreased with increasing pH from 94 % - 26 %. On the other hand, the opposite was observed for MB, whose removal efficiency increased with increasing pH, achieving its highest removal efficiency at pH 5 of 93 %. This phenomenon can be due to the transfer and removal of protons on the available functional groups on the outer part of the adsorbent under various pH conditions, as well as the anionic and cationic nature of the target dye (Kanani-jazi & Akbari, 2021). The zeta potential ($pH_{pzc}$) of the OLPAC was found to be 2.5, these denote that the surface charge of the adsorbent stays positive below the $pH_{pzc}$ and negative at pH above this value (Akawa et al., 2021a; Biata et al., 2018). So, because the OLPAC surfaces are positively charged at low pH, strong electrostatic interactions occurred between the adsorbent and the anionic MO, resulting in maximum removal efficiency. Moreover, when the pH of the solution increases to pH above the $pH_{pzc}$, the adsorbent turns out to be negatively charged and hence favoring the electrostatic interactions between the negatively charged OLPAC and the cationic MB dye. Similar results were obtained by (Baloo et al., 2021; Li et al., 2016). The optimum pH conditions for MO and MB were 2 and 6, respectively and these conditions were used in subsequent experimental studies.

Another important parameter for dye removal is a mass of adsorbent and its effect on the removal efficiencies of the MO and MB dyes on OLPAC was evaluated by measuring the adsorbent mass (0.01 g–0.8 g/50 mL), contact time: 30 min, and dye concentration: 100 mg $L^{-1}$ and optimum pH conditions for each dye. The results are shown in Figure 4(b)

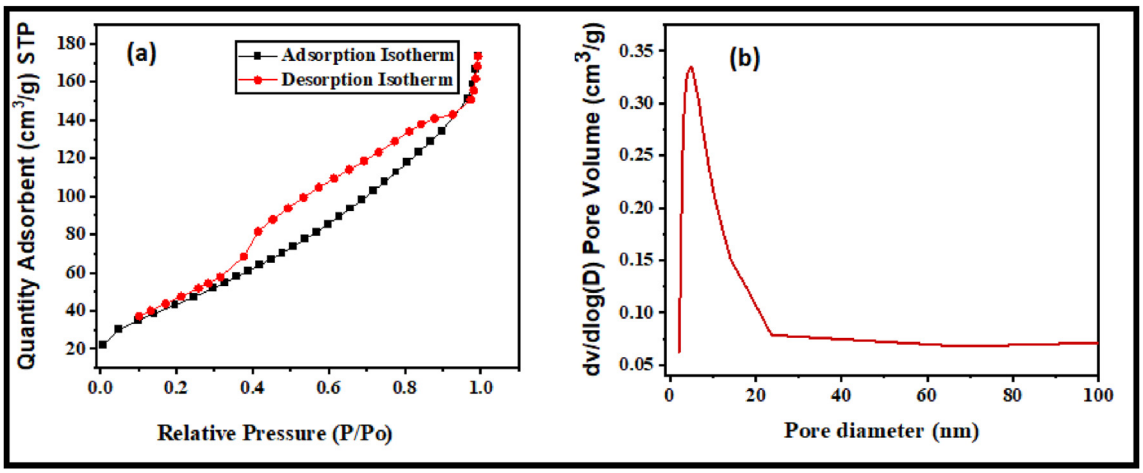


**Figure 2.** (a) BET isotherms and (b) pore size distribution curves of OLPAC.

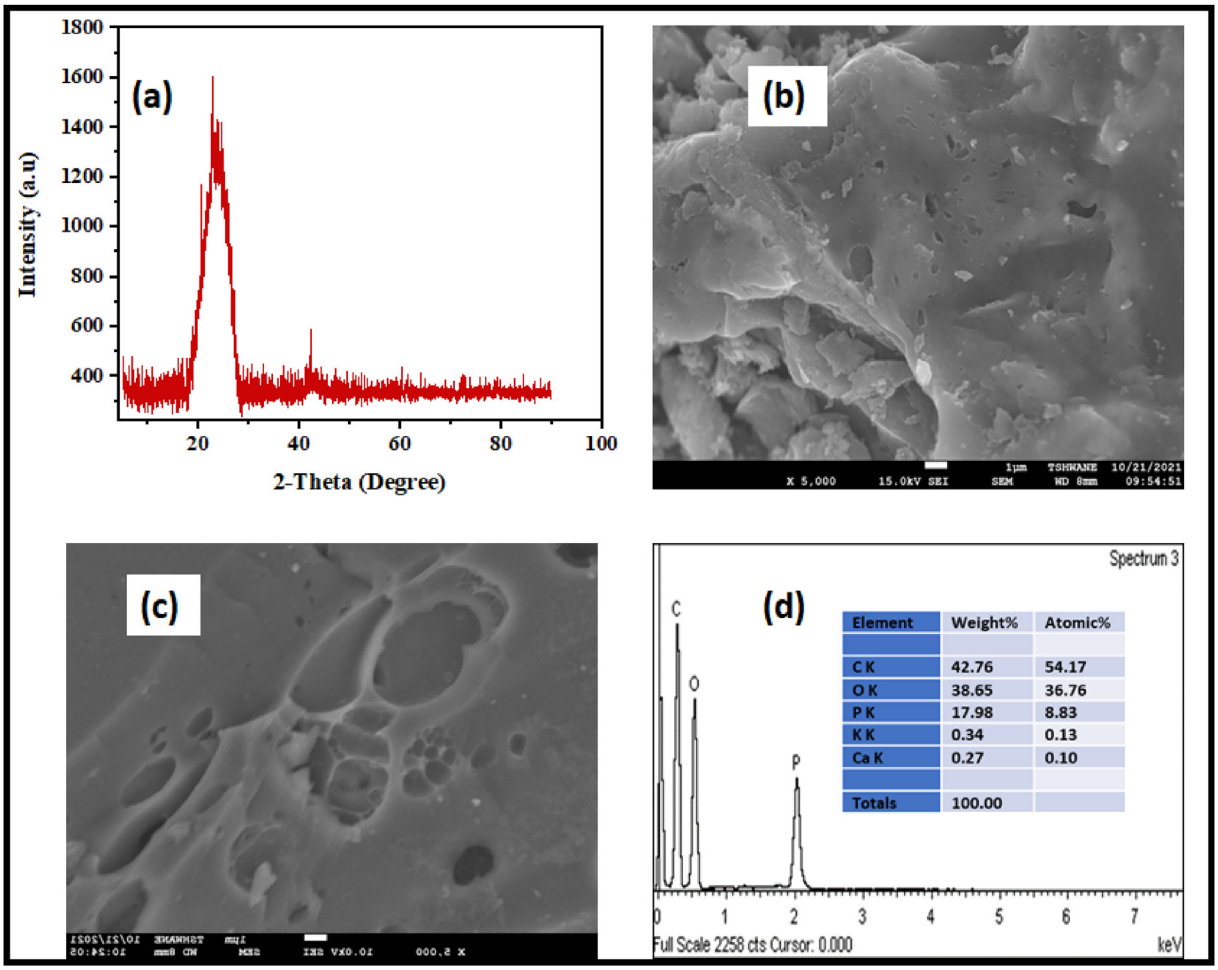


**Figure 3.** (a) XRD spectrum, (b)–(c) SEM image and (d) EDS of OLPAC.

shows a drastic increase in removal efficiency as the mass of adsorbent is varied from 0.01 g to 0.1 g. This can be attributed to the increase in surface area and available adsorption sites on the adsorbent (Zhao et al., 2022). Equilibrium and maximum adsorption efficiency were obtained at 0.2 g for both dyes and hence the optimum mass of adsorbent condition of 0.2 g was used in subsequent studies.

One more significant parameter in the wastewater treatment process is the equilibrium time. In this study, the relationship between the removal efficiency of MO and MB and contact time was explored and the results are can be seen in Figure 4(c). Figure 4(c) shows that adsorption efficiency increased with increasing contact time and gain equilibrium after 20 min and 40 min for MB and MO, respectively. The fast adsorption at first contact time was because of more available pores on the OLPAC structure which resulted in the quicker mass transfer of the dyes from the solution onto the OLPAC. Therefore, this indicates good accessibility to the binding sites for the dyes on the adsorbent which is advantageous in

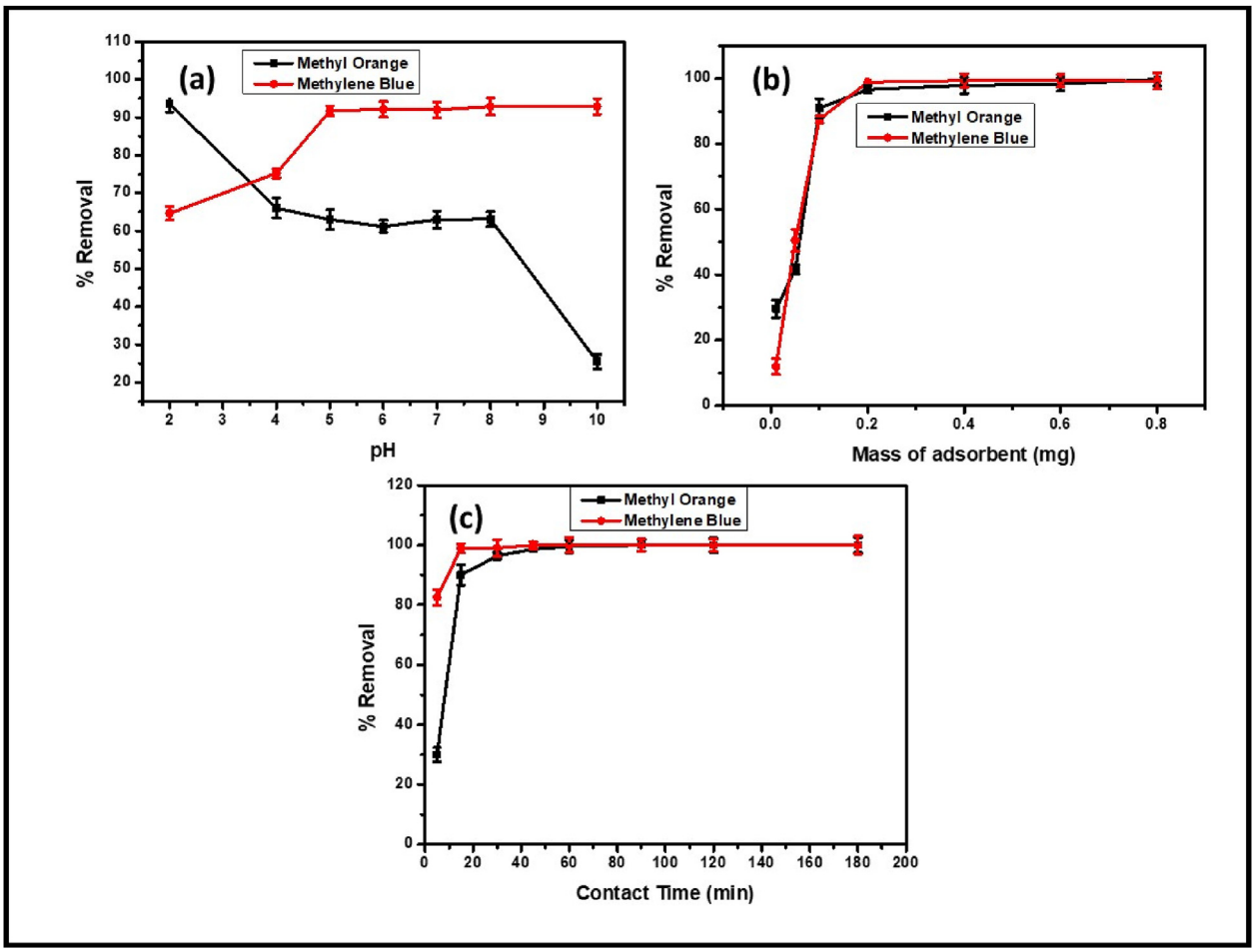


**Figure 4.** Effect of (a) sample pH, (b) adsorbent mass, and (c) contact time.

the real world as it reduces residence time (Hashemian et al., 2013; Zhao et al., 2022). The optimum conditions for contact time were 20 min and 40 min for MB and MO, respectively.

### 3.2.2. *Isotherms data analysis*

An equilibrium study was conducted to investigate the adsorption mechanisms that took place between the MO and MB dyes and the OLPAC adsorbent interaction using an adsorption isotherm model (Figure 5). The adsorption isotherm elaborate data concerning the adsorption efficiency of the adsorbent. Freundlich, Langmuir and Temkin isotherm models were used to assess the equilibrium data for the adsorption of MO and MB dyes obtained using the procedure indicated in Section 2.4.

The Langmuir isotherm adsorption model describes a monolayer retention of adsorbent atoms (molecules, ions) on a uniform surface. The Freundlich isotherm model is utilized to depict multi-facet adsorption on an adsorbent with a heterogeneous surface and the Temkin isotherm model is utilized to make sense of the direct connection between surface inclusion and adsorption heat (Cheng et al., 2021a, 2021b).

The acquired data was evaluated by the $R^2$ coefficient derived from the linear plots of the isotherm models. The representative graphs of Langmuir isotherm model are shown in Figure 6. The findings in Table 3 show that the Langmuir isotherm model fits the data well, with $R^2$ = 0.9837 and 0.9949 for MO and MB, respectively. This indicates that the adsorption of MO and MB on the surface of the adsorbent is uniform, and the coverage of the dye monolayer is dominant (Geaneth Pertunia et al., 2020; Nasrullah et al., 2018). MO and MB had the maximum adsorption capacities of 38 mg $g^{-1}$ and 33 mg $g^{-1}$, respectively. The separation factor ($R_L$) computed from the Langmuir isotherms for each dye, on the other hand, was utilized to assess if the adsorption was favorable or not. The $R_L$ value (Table 3) obtained with both dyes is less than 1, indicating good adsorption of the dye to the adsorbent (Akawa et al., 2021a; Geaneth Pertunia et al., 2020).

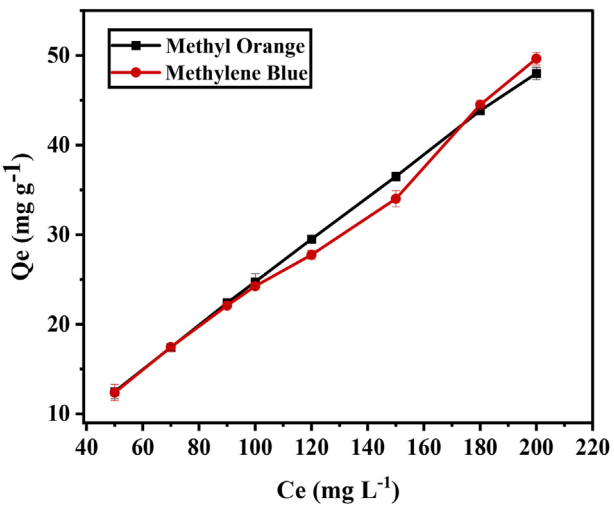


**Figure 5.** Adsorption isotherm of Methyl orange and Methylene blue on AC, (Experimental conditions: Contact time: 60 min, adsorbent mass: 0.2 g, equilibrium concentration 50–200 mg $L^{-1}$ and pH 2 and 6 for MO and MB.

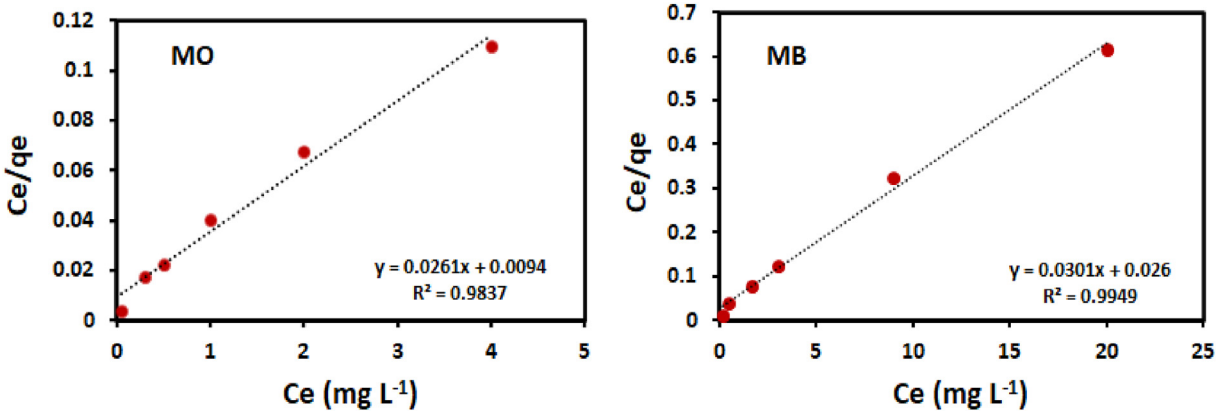


**Figure 6.** Langmuir isotherms plots for MB and MO using OLPAC.

**Table 3.** Adsorption isotherms parameters.

| Isotherms | Parameters | MO | MB |
|---|---|---|---|
| Langmuir | $q_{max}$ (mg $g^{-1}$) | 38.0 | 33.0 |
| | $K_L$ (L $mg^{-1}$) | 0.28 | 1.00 |
| | $R_L$ | 0.004 | 0.01 |
| | $R^2$ | 0.984 | 0.995 |
| Freundlich | $K_F$ | 26.15 | 31.56 |
| | n | 3.69 | 6.57 |
| | $R^2$ | 0.976 | 0.648 |
| Temkin | $K_T$ (L/g) | $3.22 \times 10^{-13}$ | 178 |
| | $B_T$ (J/mol) | 7.032 | 3.829 |
| | $R^2$ | 0.8997 | 0.8486 |

In addition, Temkin adsorption isotherm model was utilized to assess the adsorption possibilities of OLPAC adsorbent material associations and the parameters are shown in Table 3. These outcomes recommended that ßT values in adsorption processes of OLPAC material involved physical interaction (Nandiyanto et al., 2020).

### 3.2.3. Adsorption kinetics studies

A kinetic model was used to examine the adsorption mechanisms and their possible rate-determining steps (Figure 7). While the pseudo-first order depends on solid capacitance, the pseudo-second order model is successfully utilised on the sorption of analytes from aqueous solutions where chemisorption, including valence forces, occurs. This includes electron sharing or exchange between forces and adsorbents and adsorbents (Ramutshatsha-Makhwedzha et al., 2022). Table 4 shows kinetics parameters for pseudo-1st order, pseudo-2nd order, and Intra-particle diffusion the pseudo-second-order equation fits optimally for both MO and MB with an $R^2$ coefficient of 0.997 and 0.999, respectively.

The representative graphs for pseudo-second order equation are displayed in Figure 8. The results indicates that binding mechanism of pseudo-second-order prevails and adsorption of MO and MB dyes on OLPAC adsorbent is by the chemisorption step. Which has the involvement of valence force by electron exchange between the dyes and adsorbent. In addition, the half-adsorption time ($t_{1/2}$) is the required time to remove 50 % of the analyte of interest in equilibrium (Ramutshatsha-Makhwedzha et al., 2019). Moreover, the affinity between the adsorbent and the dye is high. This is reflected in the short half-adsorption time achieved with most dyes removed.

The intraparticle diffusion diagram of the adsorption of dyes by the adsorbent shows the regression line that failed to undergo the origin because C is not zero. This then counselled that each film and intra-particle diffusion affect the adsorption process.

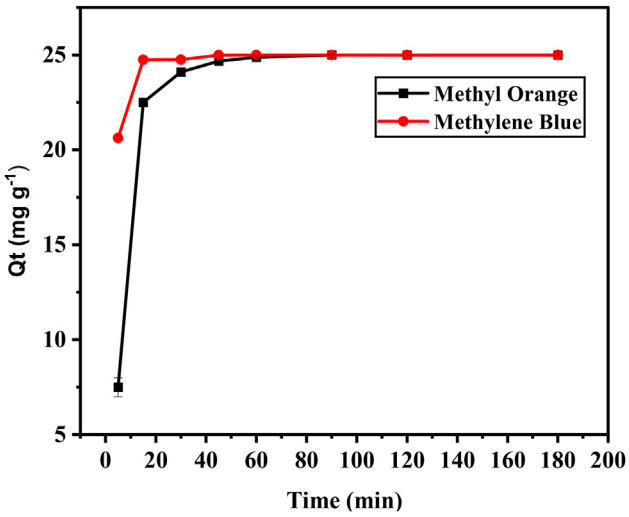


**Figure 7.** Adsorption kinetic of Methylene blue and Methyl orange on AC, (Experimental conditions: Initial concentration 100 mg $L^{-1}$, contact time 0–180 min and pH 2 and 6 for MO and MB.

**Table 4.** Kinetics parameters for pseudo-1st order, pseudo-2nd order, and Intra-particle diffusion.

| | | MO | MB |
|---|---|---|---|
| | Qe exp | 24.67 | 24.99 |
| Pseudo 1st order | $k_1$ ($min^{-1}$) | 0.106 | 0.086 |
| | $q_e$ (mg $g^{-1}$) | 12.86 | 0.03 |
| | $R^2$ | 0.673 | 0.447 |
| Pseudo 2nd order | $k_2$ (g $mg^{-1}$ $min^{-1}$) | 0.01 | 0.093 |
| | $q_e$ (mg $g^{-1}$) | 25.06 | 25.062 |
| | $R^2$ | 0.997 | 0.999 |
| | h (mg $g^{-1}min^{-1}$) | 6.28 | 58.41 |
| | $t_{1/2}$ (min) | 3.99 | 0.43 |
| Intraparticle diffusion | $k_{id1}$ (g $mg^{-1}$ $min^{-1}$) | 1.718 | 1.275 |
| | C (mg $g^{-1}$) | 8.41 | 13.191 |
| | $R^2$ | 0.618 | 0.437 |

### 3.2.4. Application for real wastewater samples

The collected wastewater samples from the laboratory were used to assess the applicability of the optimization method. The prepared OLPAC material was used to remove MO and MB from real wastewater samples. Results show that the initial concentration on real wastewater was found to be 8.8 and 12 mg $L^{-1}$ on MO and MB respectively. Table 5 shows that

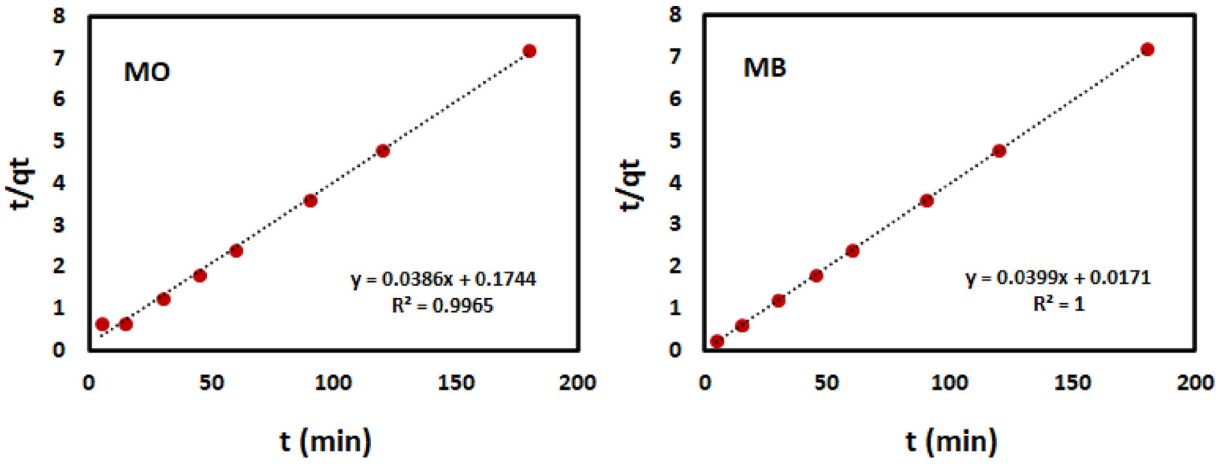


**Figure 8.** Pseudo-second order plots for MB and MO using OLPAC.

**Table 5.** Application of OLPAC on the removal of MO and MB.

| Analytes | In Con. mg $L^{-1}$ | Final Con. mg $L^{-1}$ | %Re |
|---|---|---|---|
| MO | 6 | 0.099 | 98.4 |
| MB | 2 | 0.078 | 96.1 |

**Table 6.** Summary of adsorption of dyes by activated carbon sorbents.

| Dyes | Source of Activated carbon | Adsorption capacity (mg $g^{-1}$) | Removal Efficiency (%Re) | Ref. |
|---|---|---|---|---|
| MO | Dates pits | 434 | - | (Mahmoudi et al., 2015) |
| MB | | 555 | | |
| MO | Commercial activated carbon | 113.63 | 90 | (Khattabi et al., 2021) |
| MB | Orange peels | 98.9 | 99% | (Gunay Gurer et al., 2021) |
| MB | Bamboo chip | 305.3 | 86.0 | (Jawad and Abdulhameed, 2020) |
| Acid red 18 (AR 18) | Walnut | 30.3 | >90 | (Heibati et al., 2015) |
| | Poplar woods | 3.93 | >80 | |
| MB | Nano activated carbon | 28.09 | - | (Shokry et al., 2019) |
| MO | *Prosopis juliflora* bark | 10.29 | >90 | (Kumar and Tamilarasan, 2013) |
| Azo tartrazine | commercial granular activated carbon (GAC) | 3.32 | 99.8 | (Khader et al., 2021) |
| MO | OLPAC | 33 | 98.0 | This work |
| MB | | 38 | 96.0 | |

the synthesized OLPAC adsorbent was able to remove MO and MB (%Re >96 %) on real wastewater samples.

Table 6 shows the summary of the removal of MO and MB by various agricultural precursors. In the literature study, it can be seen that ACs from different agricultural precursor have a wide scope of dye adsorption limit. For instance, Table 6 shows maximum adsorption capacities that ranges from 434–10.29 for MO and 555-28 mg $g^{-1}$ for MB, respectively. Therefore the investigated OLPAC material was comparable with the literature (Gunay Gurer et al., 2021; Heibati et al., 2015; Jawad and Abdulhameed, 2020; Khader et al., 2021; Khattabi et al., 2021; Kumar and Tamilarasan, 2013; Mahmoudi et al., 2015; Shokry et al., 2019).

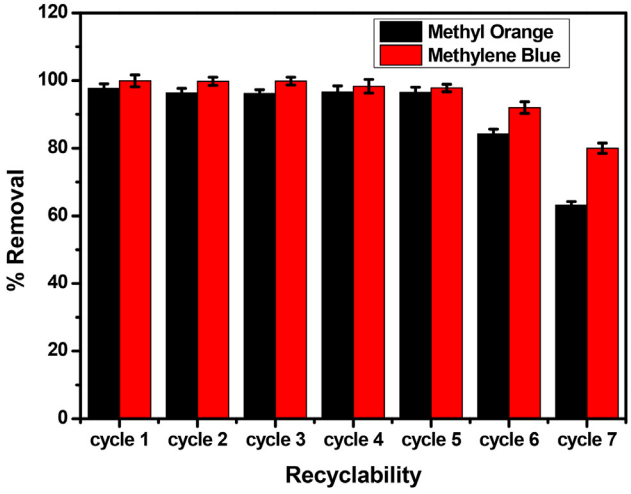


**Figure 9.** Regeneration capabilities of OLPAC.

OLPAC is a good, promising and efficient material for both MO and MB dyes from wastewater.

### 3.2.5. *Recyclability studies of the adsorbent*

Regeneration is one of the crucial factors that examines how long the adsorbents can be used. In other words, the maximum number of times an adsorbent can be used in adsorption while retaining its initial adsorption capability. The OLPAC adsorbent's reusability and stability were determined by tracking variations in % removal over time using retention–elution cycles and the results are displayed in Figure 9. The OLPAC adsorbent has been found to have consistent performance, with identical adsorption capacities up to 5 cycles and over 95 % removal efficiencies. According to the findings, the adsorbent is steady and has the potential to be used repeatedly without losing its affinity on the selected analytes.

## 4. Conclusions and future work

The application of OLPAC adsorbent was examined for the removal of MO and MB dyes from synthetic water samples. The pH and adsorbent mass were the most influential parameters on the sorption of MO and MB dye. Isotherms and kinetics results on the sorption of MO and MB dye were best described by the Langmuir isotherms and pseudo-second order reaction rate model. The obtained adsorption capacity for MO and MB was 33 and 38 mg $g^{-1}$, respectively. As a result, the electrostatic attraction was the mechanism involved between OLPAC adsorbent and

MO together with MB. While pseudo-second order suggests the chemisorption adsorption mechanism of dyes onto the OLPAC adsorbents The OLPAC material can be recovered until the fifth cycle to reuse its adsorption capacity. These could be referred to as a good cleaning technology for MO and MB adsorption. The maximum removal efficiencies of MO and MB dyes in wastewater samples ranged from 96 % to 98.4 %. Furthermore, the outcomes received shows that OLPAC nanocomposite could be a possible adsorbent for the adsorption process of MO and MB dyes.

In order to obtain basic engineering data on adsorbents for field operation, fixed-bed continuous operation is required. Further studies should focus on the application of activated carbon material derived from orange and lemon peels on continuous adsorption study using fixed-bed packed column. It is a good technology that has been previously applied in the removal of various pollutants such as methyl green and tartrazine dyes using nanocomposite material (Alardhi et al., 2020; Ali et al., 2022). Studies shows that the packed bed column offers more efficient use absorption capacity, resulting in better water quality to be treated.

## Declarations

### *Author contribution statement*

Denga Ramutshatsha-Makhwedzha: Conceived and designed the experiments; Performed the experiments; Analyzed and interpreted the data; Wrote the paper.

Avhafunani Mavhungu: Analyzed and interpreted the data; Wrote the paper.

Mapula Lucey Moropeng, Richard Mbaya: Conceived and designed the experiments; Contributed reagents, materials, analysis tools or data; Wrote the paper.

### *Funding statement*

This work was supported by Tshwane university of Technology.

### *Data availability statement*

Data will be made available on request.

### *Declaration of interests statement*

The authors declare no conflict of interest.

### *Additional information*

No additional information is available for this paper.

## Acknowledgements

Thanks to our work intergraded learning (WIL) students, LC Karume and SS Maluleke for assisting with data collection during this project.

## References

Ahmadi, S., Ganjidoust, H., 2021. Using banana peel waste to synthesize BPAC/ZnO nanocomposite for photocatalytic degradation of Acid Blue 25: influential parameters, mineralization, biodegradability studies. J. Environ. Chem. Eng. 9 (5), 106010.

Ahmed, M., Mashkoor, F., Nasar, A., 2020. Development, characterization, and utilization of magnetized orange peel waste as a novel adsorbent for the confiscation of crystal violet dye from aqueous solution. Groundwater Sustain. Dev. 10 (October 2019), 100322.

Akawa, M.N., Dimpe, K.M., Nomngongo, P.N., 2021a. An adsorbent composed of alginate, polyvinylpyrrolidone and activated carbon (AC@PVP@alginate) for ultrasound-assisted dispersive micro-solid phase extraction of nevirapine and zidovudine in environmental water samples. Environ. Nanotechnol. Monit. Manag. 16, 100559.

Akawa, M.N., Dimpe, K.M., Nomngongo, P.N., 2021b. Ultrasonic assisted magnetic solid phase extraction based on the use of magnetic waste-tyre derived activated carbon modified with methyltrioctylammonium chloride adsorbent for the preconcentration and analysis of non-steroidal anti-inflammatory drugs in. Arab. J. Chem. 14 (9), 103329.

Alardhi, S.M., Albayati, T.M., Alrubaye, J.M., 2020. Adsorption of the methyl green dye pollutant from aqueous solution using mesoporous materials MCM-41 in a fixed-bed column. Heliyon 6 (1), e03253.

Ali, M.A., Mubarak, M.F., Keshawy, M., Zayed, M.A., Ataalla, M., 2022. Adsorption of Tartrazine anionic dye by novel fixed bed Core-Shell- polystyrene Divinylbenzene/Magnetite nanocomposite. Alex. Eng. J. 61 (2), 1335–1352.

Baloo, L., Isa, M.H., Sapari, N. Bin, Jagaba, A.H., Wei, L.J., Yavari, S., Razali, R., Vasu, R., 2021. Adsorptive removal of methylene blue and acid orange 10 dyes from aqueous solutions using oil palm wastes-derived activated carbons. Alex. Eng. J. 60 (6), 5611–5629.

Biata, N.R., Dimpe, K.M., Ramontja, J., Mketo, N., Nomngongo, P.N., 2018. Determination of thallium in water samples using inductively coupled plasma optical emission spectrometry (ICP-OES) after ultrasonic assisted-dispersive solid phase microextraction. Microchem. J. 137, 214–222.

Bukhari, A., Ijaz, I., Zain, H., Gilani, E., Nazir, A., Bukhari, A., Raza, S., ansari, J., Hussain, S., Alarfaji, S.S., saeed, R., Naseer, Y., Aftab, R., Iram, S., 2022. Removal of Eosin dye from simulated media onto lemon peel-based low cost biosorbent. Arab. J. Chem. 15 (7), 103873.

Çatlıoğlu, F., Akay, S., Turunç, E., Gözmen, B., Anastopoulos, I., Kayan, B., Kalderis, D., 2021. Preparation and application of Fe-modified banana peel in the adsorption of methylene blue: process optimization using response surface methodology. Environ. Nanotechnol. Monit. Manag. 16 (April).

Cheng, S., Xing, Baolin, Shi, C., Nie, Y., Xia, H., 2021a. Efficient and selective removal of Pb(II) from aqueous solution by modification crofton weed: experiment and density functional theory calculation. J. Clean. Prod. 280, 124407.

Cheng, S., Liu, Y., Xing, B., Qin, X., Zhang, C., Xia, H., 2021b. Lead and cadmium clean removal from wastewater by sustainable biochar derived from poplar saw dust. J. Clean. Prod. 314 (December 2020), 128074.

Cheng, S., Zhao, S., Xing, B., Liu, Y., Zhang, C., Xia, H., 2022. Preparation of magnetic adsorbent-photocatalyst composites for dye removal by synergistic effect of adsorption and photocatalysis. J. Clean. Prod. 348 (September 2021), 131301.

Dey, S., Basha, S.R., Babu, G.V., Nagendra, T., 2021. Characteristic and biosorption capacities of orange peels biosorbents for removal of ammonia and nitrate from contaminated water. Cleaner Mater. 1 (April), 100001.

Dimpe, K.M., Nomngongo, P.N., 2017. A review on the efficacy of the application of myriad carbonaceous materials for the removal of toxic trace elements in the environment. Trends Environ. Anal. Chem. 16 (October), 24–31.

Eddy, N.O., Garg, R., Garg, R., Aikoye, A.O., Ita, B.I., 2022. Waste to resource recovery: mesoporous adsorbent from orange peel for the removal of trypan blue dye from aqueous solution. Biomass Convers. Biorefinery.

Fernandez, M.E., Nunell, G.V., Bonelli, P.R., Cukierman, A.L., 2014. Activated carbon developed from orange peels: batch and dynamic competitive adsorption of basic dyes. Ind. Crop. Prod. 62, 437–445.

Geaneth Pertunia, M., Kgokgobi Mogolodi, D., Philiswa Nosizo, N., 2020. A biodegradable magnetic nanocomposite as a superabsorbent for the simultaneous removal of selected fluoroquinolones from environmental water. Polymers 12, 1102.

Gugushe, A.S., Mpupa, A., Munonde, T.S., Nyaba, L., Nomngongo, P.N., 2021. Adsorptive removal of cd, cu, ni and mn from environmental samples using $Fe_3O_4$-$ZrO_2$@APS nanocomposite: kinetic and equilibrium isotherm studies. Molecules 26 (11), 3209.

Gunay Gurer, A., Aktas, K., Ozkaleli Akcetin, M., Erdem Unsar, A., Asilturk, M., 2021. Adsorption isotherms, thermodynamics, and kinetic modeling of methylene blue onto novel carbonaceous adsorbent derived from bitter orange peels. Water Air Soil Pollut. 232 (4).

Hashem, A.H., Saied, E., Hasanin, M.S., 2020. Green and ecofriendly bio-removal of methylene blue dye from aqueous solution using biologically activated banana peel waste. Sustain. Chem. Pharm. 18 (September), 100333.

Hashemian, S., Salari, K., Salehifar, H., Atashi Yazdi, Z., 2013. Removal of azo dyes (violet b and violet 5r) from aqueous solution using new activated carbon developed from orange peel. J. Chem. 2013.

Hassan, A.F., Abdel-mohsen, A.M., Elhadidy, H., 2014. Adsorption of arsenic by activated carbon, calcium alginate and their composite beads. Int. J. Biol. Macromol. 68, 125–130.

Heibati, B., Rodriguez-Couto, S., Al-Ghouti, M.A., Asif, M., Tyagi, I., Agarwal, S., Gupta, V.K., 2015. Kinetics and thermodynamics of enhanced adsorption of the dye AR 18 using activated carbons prepared from walnut and poplar woods. J. Mol. Liq. 208, 99–105.

Hijab, M., Parthasarathy, P., Mackey, H.R., Al-Ansari, T., McKay, G., 2021. Minimizing adsorbent requirements using multi-stage batch adsorption for malachite green removal using microwave date-stone activated carbons. Chem. Eng. Processing - Process Intensific. 167 (February 2020), 108318.

Jawad, A.H., Abdulhameed, A.S., 2020. Statistical modeling of methylene blue dye adsorption by high surface area mesoporous activated carbon from bamboo chip using KOH-assisted thermal activation. Energy Ecol. Environ. 5 (6), 456–469.

Jiang, Y., Qin, Z., Liang, F., Li, J., Sun, Y., Wang, X., Ma, P., Song, D., 2021. Vortex-assisted solid-phase extraction based on metal-organic framework/chitosan-functionalized hydrophilic sponge column for determination of triazine herbicides in environmental water by liquid chromatography-tandem mass spectrometry. J. Chromatogr. A 1638, 461887.

Kanani-jazi, M.H., Akbari, S., 2021. Journal of Environmental Chemical Engineering Amino-dendritic and carboxyl functionalized halloysite nanotubes for highly efficient removal of cationic and anionic dyes : kinetic , isotherm , and thermodynamic studies. J. Environ. Chem. Eng. 9 (3), 105214.

Khader, E.H., Mohammed, T.J., Albayati, T.M., 2021. Comparative performance between rice husk and granular activated carbon for the removal of azo tartrazine dye from aqueous solution. Desalination Water Treat. 229 (January 2022), 372–383.
Khattabi, E.H.E.L., Rachdi, Y., Bassam, R., Mourid, E.H., Naimi, Y., Alouani, M.E.L., Belaaouad, S., 2021. Enhanced elimination of methyl orange and recycling of an eco-friendly adsorbent activated carbon from aqueous solution. Russ. J. Phys. Chem. B 15 (S2), S149–S159.
Kooravand, M., Asadpour, S., Haddadi, H., Farhadian, S., 2021. An insight into the interaction between malachite green oxalate with human serum albumin: molecular dynamic simulation and spectroscopic approaches. J. Hazard Mater. 407 (December 2020), 124878.
Kumar, M., Tamilarasan, R., 2013. Modeling of experimental data for the adsorption of methyl orange from aqueous solution using a low cost activated carbon prepared from prosopis julifl ora. Pol. J. Chem. Technol. 15 (2), 29–39.
Li, H., Sun, Z., Zhang, L., Tian, Y., Cui, G., Yan, S., 2016. A cost-effective porous carbon derived from pomelo peel for the removal of methyl orange from aqueous solution. Colloids Surf. A Physicochem. Eng. Asp. 489, 191–199.
Madimetja, J., Nomngongo, P.N., 2019. Effective adsorptive removal of amoxicillin from aqueous solutions and wastewater samples using zinc oxide coated carbon nano fi ber composite. Emerging Contamin. 5, 143–149.
Mahmoudi, K., Hosni, K., Hamdi, N., Srasra, E., 2015. Kinetics and equilibrium studies on removal of methylene blue and methyl orange by adsorption onto activated carbon prepared from date pits-A comparative study. Kor. J. Chem. Eng. 32 (2), 274–283.
Mashile, G.P., Mpupa, A., Nomngongo, P.N., 2021. Magnetic mesoporous carbon/β-cyclodextrin–chitosan nanocomposite for extraction and preconcentration of multi-class emerging contaminant residues in environmental samples. Nanomaterials 11 (2), 1–16.
Mpupa, A., Nqombolo, A., Mizaikoff, B., Nomngongo, P.N., 2020. Enhanced adsorptive removal of β-estradiol from aqueous and wastewater samples by magnetic nano-akaganeite: adsorption isotherms, kinetics, and mechanism. Processes 8 (9), 1–18.
Nandiyanto, A.B.D., Arinalhaq, Z.F., Rahmadianti, S., Dewi, M.W., Rizky, Y.P.C., Maulidina, A., Anggraeni, S., Bilad, M.R., Yunas, J., 2020. Curcumin adsorption on carbon microparticles: synthesis from soursop (annonamuricata l.) peel waste, adsorption isotherms and thermodynamic and adsorption mechanism. Int. J. Nanoelectr. Mater. 13 (Special issue), 173–192.
Nasrullah, A., Bhat, A.H., Naeem, A., Hasnain, M., 2018. High surface area mesoporous activated carbon-alginate beads for efficient removal of methylene blue. Int. J. Biol. Macromol. 107, 1792–1799.
Ngah, W.S.W., Teong, L.C., Hanafiah, M.A.K.M., Wan Ngah, W.S., Teong, L.C., Hanafiah, M.A.K.M., 2011. Adsorption of dyes and heavy metal ions by chitosan composites: a review. Carbohydr. Polym. 83 (4), 1446–1456.
Olivera, S., Basavarajaiah, H., Venkatesh, K., Kumar, V., Gopalakrishna, K., K, Y.K., Muralidhara, H.B., Venkatesh, K., Guna, V.K., Gopalakrishna, K., Kumar, K.,Y., 2016. Potential applications of cellulose and chitosan nanoparticles/composites in wastewater treatment: a review. Carbohydr. Polym. 153, 600–618.
Pandiarajan, A., Kamaraj, R., Vasudevan, S., Vasudevan, S., 2018. OPAC (orange peel activated carbon) derived from waste orange peel for the adsorption of chlorophenoxyacetic acid herbicides from water: adsorption isotherm, kinetic modelling and thermodynamic studies. Bioresour. Technol. 261 (April), 329–341.
Parlayıcı, Ş., Pehlivan, E., 2021. Biosorption of methylene blue and malachite green on biodegradable magnetic Cortaderia selloana flower spikes: modeling and equilibrium study. Int. J. Phytoremediation 23 (1), 26–40.
Ramutshatsha-Makhwedzha, D., Mbaya, R., Mavhungu, M.L., 2022. Application of activated carbon banana peel coated with $Al_2O_3$-chitosan for the adsorptive removal of lead and cadmium from wastewater. Materials 15 (3).
Ramutshatsha-Makhwedzha, D., Ngila, J.C., Ndungu, P.G., Nomngongo, P.N., 2019. Ultrasound assisted adsorptive removal of Cr, Cu, Al, Ba, Zn, Ni, Mn, Co and Ti from seawater using $Fe_2O_3$-$SiO_2$-PAN nanocomposite: equilibrium kinetics. J. Mar. Sci. Eng. 7 (5).
Shokry, H., Elkady, M., Hamad, H., 2019. Nano activated carbon from industrial mine coal as adsorbents for removal of dye from simulated textile wastewater: operational parameters and mechanism study. J. Mater. Res. Technol. 8 (5), 4477–4488.
Singh, S., Parveen, N., Gupta, H., 2018. Adsorptive decontamination of rhodamine-B from water using banana peel powder: a biosorbent. Environ. Technol. Innovat. 12, 189–195.
Tan, K.A., Morad, N., Teng, T.T., Norli, I., Panneerselvam, P., 2012. Removal of cationic dye by magnetic nanoparticle ($Fe_3O_4$) impregnated onto activated maize cob powder and kinetic study of dye waste adsorption. APCBEE Procedia 1 (January), 83–89.
Wong, S., Ngadi, N., Inuwa, I.M., Hassan, O., 2018. Recent advances in applications of activated carbon from biowaste for wastewater treatment: a short review. J. Clean. Prod. 175, 361–375.
Yagub, M.T., Sen, T.K., Afroze, S., Ang, H.M., 2014. Dye and its removal from aqueous solution by adsorption: a review. In: Advances in Colloid and Interface Science.
Zhang, W., Wang, Y., Fan, L., Liu, X., Cao, W., Ai, H., Wang, Z., Liu, X., 2022. Sorbent Properties of Orange Peel-Based Biochar for Different Pollutants in Water.
Zhao, W., Zhao, Y., Zhang, H., Hao, C., Zhao, P., 2022. Efficient removal of cationic and anionic dyes by surfactant modified $Fe_3O_4$ nanoparticles. Colloids Surf. A Physicochem. Eng. Asp. 633 (P1), 127680.